

# Deconvolving Spectra of Lensing Galaxies, QSO Hosts, and More . . .

F. COURBIN<sup>1,2</sup>, P. MAGAIN<sup>2\*</sup>, S. SOHY<sup>2</sup>, C. LIDMAN<sup>3</sup>, G. MEYLAN<sup>4</sup>

<sup>1</sup>Universidad Católica de Chile, Departamento de Astronomía y Astrofísica, Santiago, Chile

<sup>2</sup>Institut d'Astrophysique et de Géophysique, Liège, Belgium

<sup>3</sup>European Southern Observatory, Chile

<sup>4</sup>European Southern Observatory, Garching

\*Also Maître de recherches au FNRS (Belgium)

## 1. Background and Motivation

High spatial resolution undoubtedly plays a key role in most major advances in observational astrophysics. In this context, considerable effort has been devoted to the development of numerical methods aimed at improving the spatial resolution of astronomical images. However, the most commonly used techniques (e.g., Richardson 1972, Lucy 1974, Skilling & Bryan 1984) tend to produce the so-called “deconvolution artefacts” (oscillations in the vicinity of high spatial frequency structures) which alter the photometric and astrometric properties of the original data. Recently, Magain, Courbin & Sohy (1998ab; hereafter MCS) proposed and implemented a new deconvolution algorithm which overcomes such drawbacks. Its success is mainly the consequence of a deliberate choice to achieve an improved resolution rather than an infinite one, hence avoiding retrieving spatial frequencies forbidden by the sampling theorem.

Many successful applications of the MCS algorithm have been carried out in

the framework of an intensive effort to obtain detailed light/mass maps for lensing galaxies (e.g., Courbin et al. 1997, 1998ab, Burud et al. 1998abc). These results, when compared with recent Hubble Space Telescope (HST) images, clearly demonstrate the effectiveness of the method in producing reliable high-resolution images.

High angular resolution is certainly a must in imaging, but it is also of great interest in spectroscopy. From realistic simulations, we illustrate here a promising spectroscopic version of the MCS algorithm. We demonstrate that flux-calibrated spectra of severely blended objects can be accurately extracted and show how the algorithm can be used to decontaminate the spectra of extended objects from the light of very nearby bright point sources. The preliminary deconvolution of near-IR NTT (SOFI) spectra of the lensed QSO HE 1104-1805 are presented as an example of an application to real data. The faint spectrum of the lensing galaxy is clearly unveiled by the deconvolution algorithm.

## 2. Spatial Deconvolution of Spectra

MCS have shown that sampled images should not be deconvolved with the observed Point Spread Function (PSF), but with a narrower function, chosen so that the final deconvolved image can be properly sampled, whatever sampling step is adopted to represent it. For this purpose, one chooses the final (well-sampled) PSF of the deconvolved image and computes the PSF which should be used to perform the deconvolution and which replaces the observed total PSF.

Depending on the resolution which is aimed at, the width of such a profile may be anything between “slightly narrower” than the observed PSF or seeing (this results in a very high but not infinite gain in resolution), and critically sampled width, which would result in a modest gain in resolution. A straightforward consequence of choosing the shape that the PSF will have in the deconvolved image is that it is, indeed, exactly known. Such prior knowledge can be used to decompose the data (image or spectrum) into a sum of point

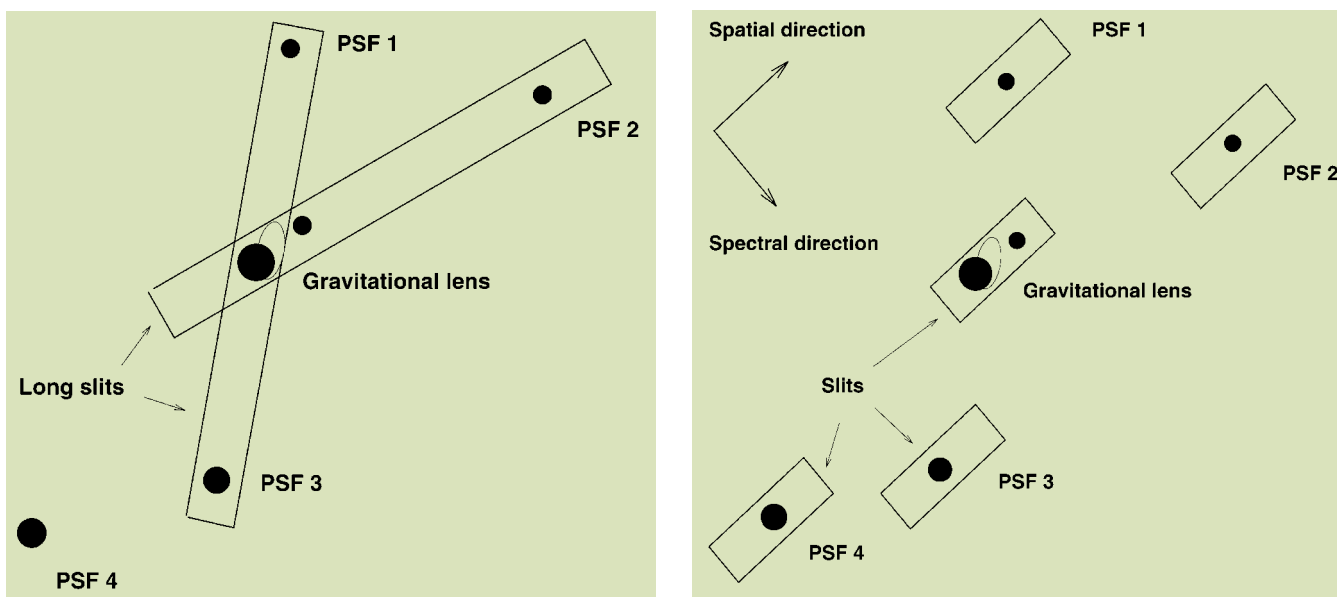


Figure 1: Two possible instrumental set-ups to obtain simultaneously the spectra of the object of scientific interest (a lensed QSO in the present example) and that of one or more PSF stars. Left: long slit spectroscopy. Right: Multi Object Spectroscopy. The latter allows one to observe several PSF stars, whatever Position Angle is selected to observe the target.

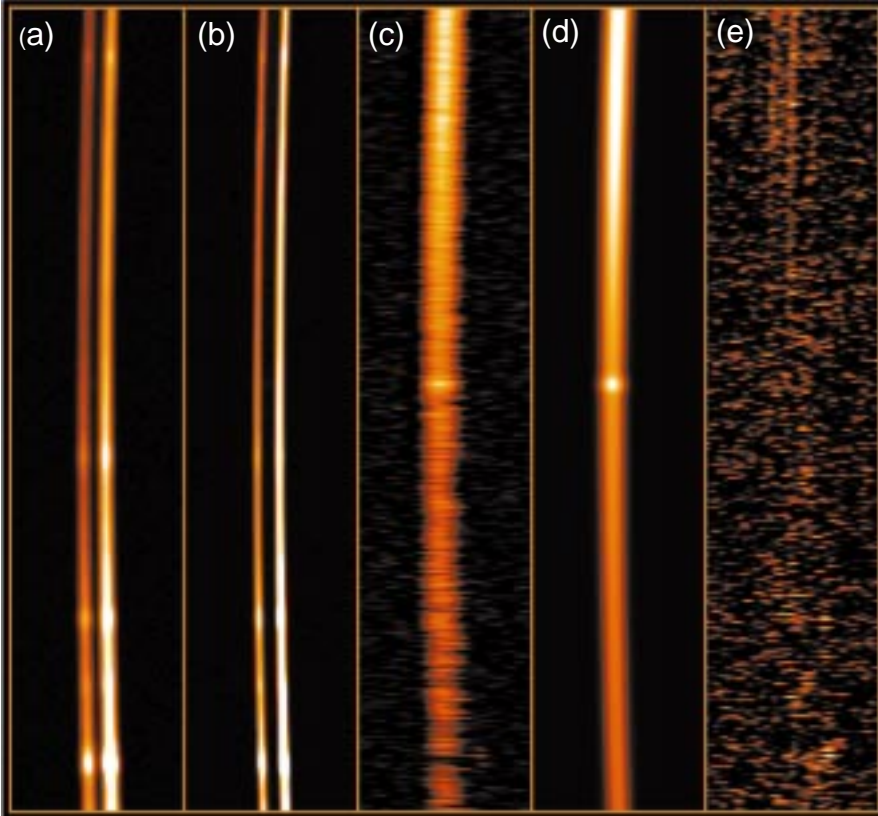


Figure 2: From left to right: (a) Simulated spectrum of a lensed quasar ( $\sim 4000\text{--}8000 \text{ \AA}$ ), (b) its deconvolution, (c) the deconvolved background (here, the lensing galaxy alone), (d) the galaxy used to construct the simulation, and (e) the residual image (data minus model) in units of the photon noise. The simulation considers seeing variation with wavelength and (exaggerated) atmospheric refraction.

sources with known analytical spatial profile, and deconvolved numerical background. This decomposition was successfully used in the MCS image deconvolution algorithm. We applied the same fundamental rule to construct an algorithm for the spatial deconvolution of spectra, as described in detail in Courbin, Magain, Kirkove & Sohy (1999).

As with the image deconvolution algorithm, precise knowledge of the instrumental profile is required. This profile varies with wavelength and time. It may be obtained in practice by aligning simultaneously on the slit, both the object of scientific interest and one or several point sources. Whenever the target is multiple (this is indeed likely if deconvolution is required), no reference point source may be observable on the same slit, as the position angle of the spectrograph is in such a case imposed by the geometry of the target. This is no more true when observing in MOS mode, where several PSF stars can be observed at the same time and used to improve the spatial sampling of the spectra, to reach even higher spatial resolution and to achieve more accurate point/extended sources decomposition. Then, finding suitable PSF stars is not more a limitation in spectroscopy than in imaging. Figure 1 shows two examples of instrumental set-ups which may be adopted to yield observations well suited to the problem of spectra deconvolution.

In order to minimise the effect of the PSF variation across the field, PSF stars should be selected as close to the main target as possible. Observing several such point sources will not only allow oversampling of the deconvolved spectra, but also to check whether a given reference star is multiple or not, and to check the PSF stability over the field. Even if the algorithm can cope with critically sampled data, detectors with small pixel sizes should be preferred (e.g., the high-resolution collimator of FORS1/FORS2 provides  $0.1''$  pixel, which is exceptionally small for a spectrograph), and high signal-to-noise ratio aimed at. The above conditions are in fact the same as in imaging. Good sampling, PSF stability and high signal-to-noise are definitely the main requirements when performing photometrically (spectrophotometrically in the present case) accurate deconvolutions.

In practise, the deconvolved PSF (i.e., shape of the point sources in the deconvolved spectra) can be as narrow as one may wish, the only theoretical limitation to the gain in resolution being the sampling of the deconvolved data. In our implementation of the algorithm, one can improve the pixel size (in the spatial direction) by a factor 2, so that the maximum resolution will be 2 (half) CCD pixels FWHM. This limit can in principle be reached, whatever seeing is available in the data spectra, although,

as one can expect, the quality of the result decreases as the seeing increases.

### 3. Simulations

The algorithm has two obvious applications: firstly, to extract the individual spectra of strongly blended point sources and, secondly, to unveil the spectra of extended objects hidden by much brighter point sources. While de-blending point sources is relatively easy (see Courbin, Magain, Kirkove & Sohy 1999 for an example), the most interesting applications of our spectrum deconvolution algorithm may consist in its capability to decompose spectra into the components from point sources and extended sources. The two simulated spectra presented hereafter illustrate the results that can be expected from high signal-to-noise data.

Our simulations include slit misalignment, seeing variation as a function of wavelength as well as – exaggerated – atmospheric refraction. Gaussian photon noise and readout noise are also added to the data. A typical signal-to-noise ratio is 200–300 per spectral-resolution element. The PSF is derived from the simulated spectrum of a point source whose S/N ratio is similar to the one of the scientific data. The deconvolutions are performed as in imaging and the optimal choice of the different Lagrange multipliers to be used is guided by the visual inspection of the residual maps (RM) (see Burud et al. 1998b for an example of a RM). The RM is the absolute value of the difference between the raw data and the deconvolved image reconvolved by the (narrower) PSF, in units of the noise. An accurate deconvolution should therefore correspond to a flat RM with a mean value of 1.

#### 3.1 Simulated lens and QSO host galaxies

Figure 2 presents the simulated spectra of two lensed images of the same quasar, separated by 6 pixels in the spatial direction. The spatial resolution is 4 pixels FWHM and the signal-to-noise ratio of the brightest spectrum is about 200–300 per spectral resolution element, depending on the wavelength. The flux ratio between the two QSO images is 3 (1.2 magnitudes). The spectrum of the – extended – lensing galaxy is also incorporated in the simulated data. It is located only 2 pixels away from the centroid of the faintest QSO image and is about 3 to 5 magnitudes fainter than the QSO images (depending on wavelength) and therefore completely invisible in the raw data (see left panel of Figure 2). The second panel shows the result of the deconvolution, the third panel displays the 2-D deconvolved spectrum of the lensing galaxy alone, which compares very well with the original simulated spectrum shown in the fourth panel. The RM, as defined at the beginning of this section, is displayed

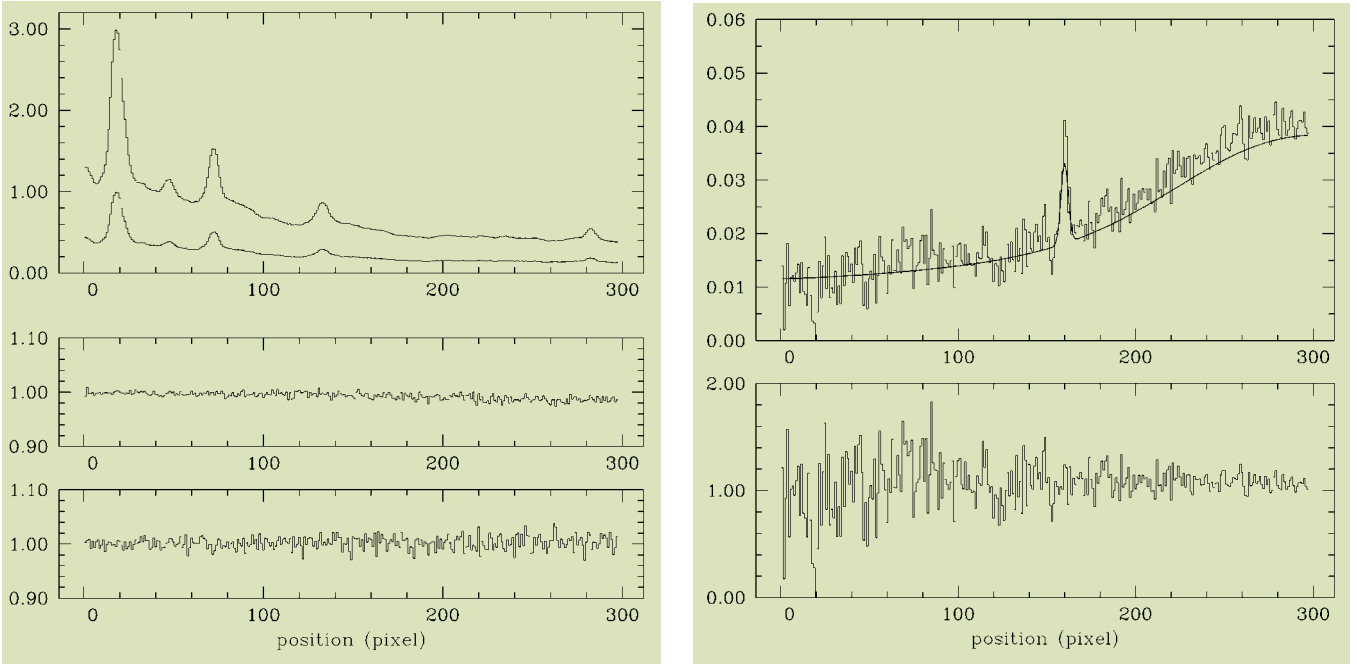


Figure 3: **Left:** The top panel shows the 1-D deconvolved spectra of the two simulated QSO images. In the middle and bottom panels are displayed the flux ratios between the two spectra and the original QSO spectrum used in the simulation. **Right:** the spectrum of the lensing galaxy alone (top) and its division by the input spectrum (bottom). The position of the emission line is retrieved with an accuracy of 0.1 pixel.

in the last panel and does not show any significant structure, as expected for a good deconvolution.

Figure 3 confirms the good results obtained in Figure 2. The 1-D spectra of the 2 QSO images as well as the spectrum of the lensing galaxy are in very good agreement with the input spectra (solid line), in spite of the blending and high luminosity contrast. The emission line in the spectrum of the lensing galaxy is well recovered and its (spectral) position is retrieved with an accuracy of 0.1 pixel.

A more difficult application may consist of the spectroscopic study of QSO host galaxies. In this case, a bright QSO is centred almost exactly on the bulge of a much fainter host galaxy, which can sometimes be imaged with standard techniques. We have tested the spectroscopic version of the MCS algorithm on such a difficult case, and show from the results in Figure 3 that the spectrum of a host galaxy can be accurately decontaminated from light pollution by its central AGN. The host galaxy in our example is

about 2 magnitudes fainter than the QSO and has the spatial extension of a low redshift galaxy ( $z = 0.1-0.3$ ).

### 3.2 A near-IR spectrum of the lensing galaxy in HE 1104–1805

We recently obtained with SOFI, mounted on the NTT, near-IR spectra of the so-called “double Hamburger”, i.e., the doubly imaged gravitationally lensed QSO HE 1104–1805 (Wisotzki et al. 1993), discovered in the Hamburg survey for bright

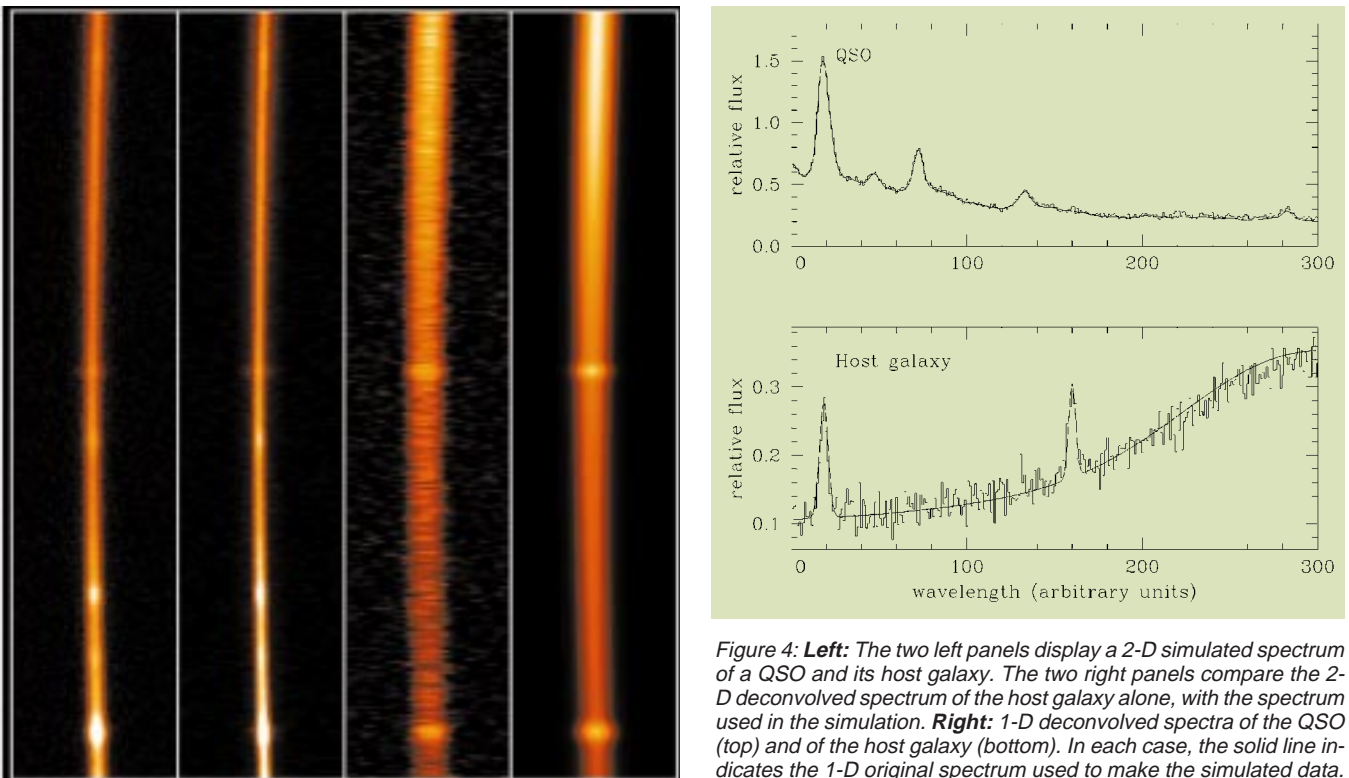


Figure 4: **Left:** The two left panels display a 2-D simulated spectrum of a QSO and its host galaxy. The two right panels compare the 2-D deconvolved spectrum of the host galaxy alone, with the spectrum used in the simulation. **Right:** 1-D deconvolved spectra of the QSO (top) and of the host galaxy (bottom). In each case, the solid line indicates the 1-D original spectrum used to make the simulated data.

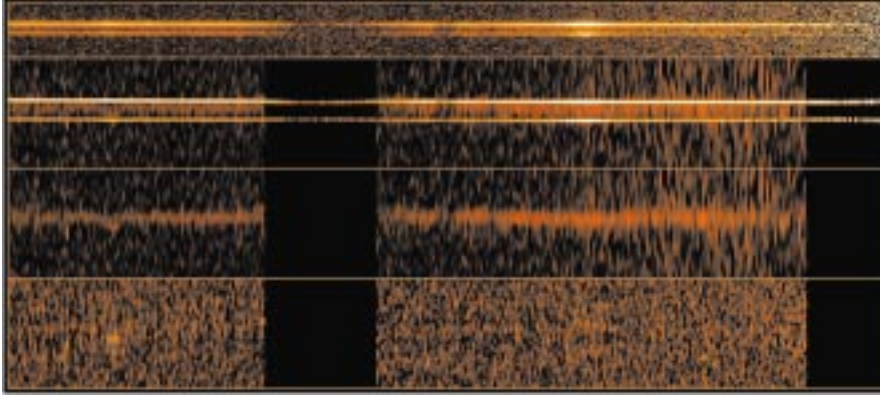


Figure 5: From top to bottom: A near-IR spectrum of the lensed QSO HE 1104–1805, between 1.5  $\mu\text{m}$  (left) and 2.5  $\mu\text{m}$  (right). The seeing is 0.6–0.7 arcsec and the lensing galaxy is situated about 0.5'' away from the brightest QSO image. The spectrum is deconvolved down to a resolution of 0.3'' with improvement of the sampling in the spatial direction. The third panel displays the spectrum of the lens alone and the last panel shows the residual map (RM, see text) in unit of the photon noise, to illustrate the good agreement between the data and their deconvolution. The dark areas are not used, because of strong atmospheric absorption.

QSOs and for which the time delay has been reported (Wisotzki et al. 1998). However, the redshift of the main lensing galaxy remains unknown, which still hampers any attempt to estimate  $H_0$  from this system. As the lensing galaxy is very red (e.g., Courbin et al. 1998b), near-IR spectroscopy appeared an obvious way of determining its redshift.

SOFI spectra were obtained at the NTT between 0.9 and 2.5 microns under good seeing conditions (about 0.6–0.7'') and deconvolved down to a resolution of 0.3''. As no PSF star was observed, the PSF was computed directly from the spectra of the two QSO images (more details about this procedure are given in Courbin et al. 1999). Figure 4 shows the results of the deconvolution performed between 1.5 and 2.5 microns, since the lens is too faint in the 0.9–1.5 micron region. The original data are shown in the top panel of Figure 4. The three other panels, from top to bottom, show the deconvolved spectra with improved sampling (0.145''/pixel) in the spatial direction (this is why the width of the deconvolved 2-D images is twice that of the raw data), the spectrum of the lensing galaxy, as well as the RM (flat with a mean value of 1). The data presented here have a much

lower S/N than in the simulations but are sufficient to unveil the spectrum of the faint lens. Since no emission line is detected, we are still left without precise measurement of the lens redshift. However, the prospect of measuring this redshift with optical/near-IR spectroscopy is good: with the improved S/N, sampling, and spectral resolution of future VLT data!

#### 4. Future Prospects

Our new extension to spectroscopy of the MCS image deconvolution algorithm obviously has a wide field of applications. The most original and promising ones may consist in spectroscopic studies involving extended objects hidden by – often brighter – point sources. We have presented an application of the method to gravitationally lensed quasars, where the spectrum of a very faint lensing galaxy can be extracted. A similarly interesting application will be to take full advantage of the ability of the algorithm to decompose spectra, in order to carry out the first systematic spectroscopic study of quasar host galaxies. With current instrumentation mounted on 8–10-m-class telescopes, sufficiently high signal-to-noise spectra can be obtained, at least for low-

redshift quasars, in order to derive precise rotation curves of their host galaxy, provided the spectrum of the bright QSO nucleus can be removed accurately. The present spectrum deconvolution algorithm is very well suited for such a purpose and may therefore allow significant progress, not only towards the measurement of the mass of the central black hole in QSO host galaxies, but also in astrophysics in general. We intend to release in the near future a documented public version of our image deconvolution algorithms, followed later by the spectroscopic version of code illustrated in the present article.

#### Acknowledgements

F. Courbin acknowledges financial support through the Chilean grant FONDECYT/3990024. S. Sohy is supported by contracts ARC 94/99–178 ‘‘Action de Recherche Concertée de la Communauté Française (Belgium)’’ and ‘‘Pôle d’Attraction Interuniversitaire’’ P4/05 (SSTC Belgium).

#### References

- Burud, I., Courbin, F., Lidman, C., et al. 1998a, *ApJ*, **501**, L5.
- Burud, I., Courbin, F., Lidman, C., et al. 1998b, *The Messenger* **92**, 29.
- Burud, I., Stabell, R., Magain, P., et al. 1998c, *A&A*, **339**, 701.
- Courbin, F., Magain, P., Keeton, C.R., et al. 1997, *A&A*, **324**, L1.
- Courbin, F., Lidman, C., Frye, B., et al. 1998a, *ApJ*, **499**, L119.
- Courbin, F., Lidman, C., Magain, P., 1998b, *A&A* **330**, 57.
- Courbin, F., Magain, P., Kirkove, M., Sohy, S., 1999, *ApJ*, in press.
- Courbin, F., Lidman, C., Meylan, G., Magain, P., 1999, in preparation.
- Lucy, L. 1974, *AJ*, **79**, 745.
- Magain, P., Courbin, F., & Sohy, S. 1998a, *ApJ*, **494**, 472.
- Magain, P., Courbin, F., & Sohy, S. 1998b, *The Messenger* **88**, 28.
- Richardson, W.H.J. 1972, *J. Opt. Soc. Am.*, **62**, 55.
- Skilling, J., & Bryan, R.K. 1984, *MNRAS*, **211**, 111.
- Wisotzki, L., Koehler, T., Kayser, R., Reimers, D., 1993, *A&A* **278**, L15.
- Wisotzki, L., Wucknitz, O., Lopez, S., Sorensen, A., 1998, *A&A* **339**, L73.

## Emission-Line-Object Survey in the LMC with the WFI: New Faint Planetary Nebulae

P. LEISY<sup>1</sup>, P. FRANCOIS<sup>1,2</sup>, and P. FOUQUÉ<sup>1,3</sup>

<sup>1</sup>European Southern Observatory, Santiago, Chile; <sup>2</sup>Observatoire Meudon DASGAL, Paris, France

<sup>3</sup>Observatoire Meudon DESPA, Paris, France

### 1. Introduction

Until now, all emission-line-object surveys in the two Magellanic Clouds (MCs)

have been made with Schmidt plates, either with prism objective or with the 2-filter (ON, OFF) method. The only deep survey, dedicated to the central part of the

MCs, dates from 1980, and suffers from large biases because it was done using only two filters to select the candidates (about 30% of false candidates). No